

# Three-load Cyclic Controlled Single-Stage AC-AC Resonant Converter for Induction Cooking Applications

Srinivas Khatroth

Department of Electrical Engineering  
National Institute of Technology  
Warangal, Telangana, India  
srinukhithu@student.nitw.ac.in

Porpandiselvi S

Department of Electrical Engineering  
National Institute of Technology  
Warangal, Telangana, India  
selvi@nitw.ac.in

Vishwanathan N

Department of Electrical Engineering  
National Institute of Technology  
Warangal, Telangana, India  
nvn@nitw.ac.in

**Abstract**—This paper presents single-stage AC-AC resonant converter for three load induction cooking (IC) applications. The proposed work features power factor correction, boost operation and independent power control of loads. In this work cyclic control technique is used for independent power control. Three legs of the inverter are used to power three loads. Number of switching devices per load is two. ZVS operation is achieved for load variation of wider range and high converter is obtained. The developed approach has fewer components and uses one leg per load on average. It may also be expanded to accommodate more than three loads.

**Index Terms**—Single-stage, Resonant converter, multiple load, Induction cooking.

## I. INTRODUCTION

Induction Heating (IH) is widely used in domestic cooking applications compared to other conventional heating methods due to compatibility, controllability, reliability and environmental friendly. In literature, various converter configurations are proposed [1]–[3], like multi-stage and single-stage converter topologies for single load and multiple load IC applications. Multi-stage multiple load resonant inverter configurations are popular [4], [5] due less component count, high efficiency and independent control. Power control of these configurations are achieved through pulse frequency modulation, asymmetric duty cycle control (ADC), asymmetric voltage cancellation, phase shift control (PS) and pulse density modulation (PDM) [6]–[10] and other different control techniques. These control techniques have there own advantages and limitations. In the past literature, most of the single-stage converter configurations available are suitable for single load IC applications. Few single-stage converter topologies are proposed for multiple-load IC applications. These multi load configurations are well suitable for domestic induction cooking due to unity power factor, boost operation and high efficiency [11]–[16]. These converter configurations have there own merits and demerits. In [17], a direct ac-ac matrix converter is used to supply multiple IH but this has a drawback of increased current harmonics. A multi-phase resonant inverter with vertically aligned coupled coil

[18] improves power capability of the system with phase shift control.

In this paper, a three leg cyclic controlled single-stage resonant ac-ac converter configuration is proposed which is suitable for three IH loads. These loads are connected across the three legs in delta manner. Independent power control of respective load is achieved by ‘cyclic control’. In this technique, On-Off of inverter legs are connected in cyclic way. The benefits that can be drawn from this converter are bridge less rectifier, unity power factor, boost operation and reduced number of legs per load. Independent control of three loads is also provided.

## II. PROPOSED CONFIGURATION

### A. Circuit Description

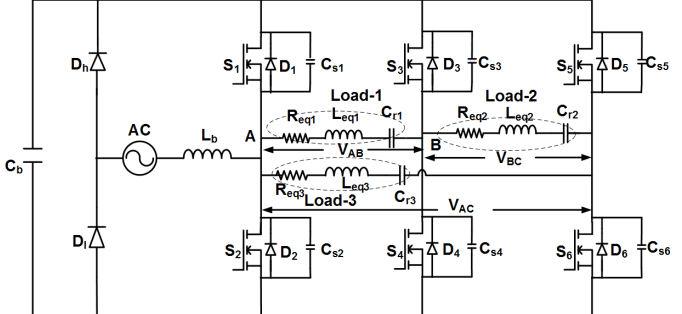


Fig. 1. Circuit diagram of single-stage three load converter

Single-stage resonant converter configuration has been proposed for three load domestic IC application. The circuit diagram of proposed converter is shown in Fig.1. The converter structure consists of a boost inductor  $L_b$ , and a small value of dc link capacitor  $C_b$  linked in such a manner that the utility frequency source voltage  $V_s$  is increased.  $v_b$  is the voltage across dc-link capacitor  $C_b$ . Diodes  $D_h$  and  $D_l$  form the rectifier branch and three legs of the resonant inverter supply power to three loads. Leg-1 switching devices  $S_1$ ,  $S_2$  and

their anti parallel diodes  $D_1$  and  $D_2$  supply power to load-1. The parameters of load-1 are equivalent resistance  $R_{eq1}$  and equivalent inductance  $L_{eq1}$ . In order to resonate the load, external resonant capacitor  $C_{r1}$  is selected in such a way to make resonant load little inductive. Hence ZVS operation is achieved with snubber capacitor  $C_{s1}$  and  $C_{s2}$ . Leg-2 switches  $S_3$ ,  $S_4$  and their anti parallel diodes  $D_3$  and  $D_4$  supply power to load-2. The parameters of load-2 are equivalent resistance  $R_{eq2}$  and equivalent inductance  $L_{eq2}$ . In order to resonate the load, external resonant capacitor  $C_{r2}$  is selected in such a way to make resonant load little inductive. Hence ZVS operation is achieved with snubber capacitor  $C_{s3}$  and  $C_{s4}$ . Leg-3 switches  $S_5$ ,  $S_6$  and their anti parallel diodes  $D_5$  and  $D_6$  supply power to load-3. The parameters of load-3 are equivalent resistance  $R_{eq3}$  and equivalent inductance  $L_{eq3}$ . In order to resonate the load, external resonant capacitor  $C_{r3}$  is selected in such a way to make resonant load little inductive. Hence ZVS operation is achieved with snubber capacitor  $C_{s5}$  and  $C_{s6}$ . IH loads are connected in delta manner with three legs of the resonant converter.

### III. MODES OF OPERATION

#### A. Cyclic control

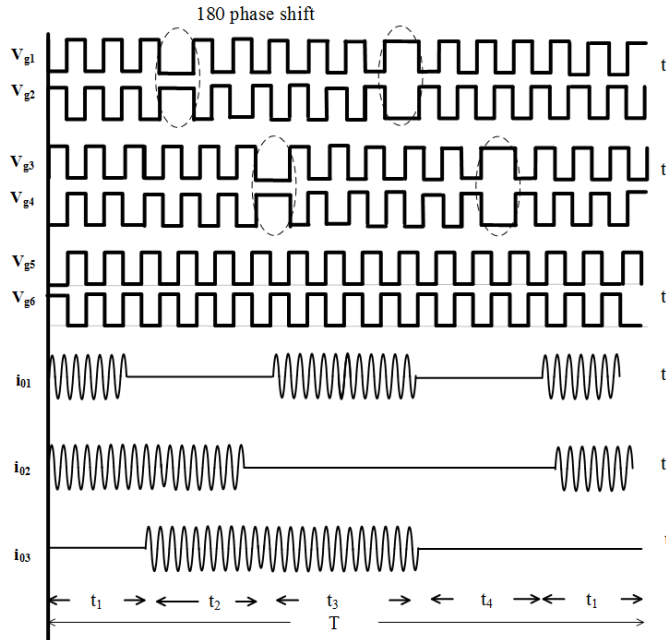


Fig. 2. Control pulses and load current waveforms

Operation of the proposed converter configuration is explained through eight modes based on the output voltage. Three loads are considered.  $T$  is the operation period. This period is divided into four intervals  $t_1$ ,  $t_2$ ,  $t_3$  and  $t_4$ . Hence  $T = t_1 + t_2 + t_3 + t_4$ .

Mode-1: Switching pulses to  $S_1$ ,  $S_4$  and  $S_5$  are in phase and this operation is shown in Fig.3a. Time interval of this mode is  $t_1$ . During this interval voltage across load-1 and load-2 are  $V_b$  and voltage across load-3 is zero.

Mode-2: Switching pulses to  $S_2$ ,  $S_4$  and  $S_5$  are in phase and this operation is shown in Fig.3b. Time interval of this mode is  $t_2$ . During this interval voltage across load-2 and load-3 are  $V_b$  and voltage across load-1 is zero.

Mode-3: Switching pulses to  $S_3$ ,  $S_4$  and  $S_5$  are in phase and this operation is shown in Fig.3c. Time interval of this mode is  $t_3$ . During this interval voltage across load-1 and load-3 are  $V_b$  and voltage across load-2 is zero.

Mode-4: Switching pulses to  $S_1$ ,  $S_3$  and  $S_5$  are in phase and this operation is shown in Fig.3d. Time interval of this mode is  $t_4$ . During this interval voltage across load-1, load-2 and load-3 is zero.

load-1 total powering time =  $t_1 + t_2$

load-2 total powering time =  $t_2 + t_3$

load-3 total powering time =  $t_1 + t_3$

Depending on the power requirement of the different loads, there may be an interval 't<sub>4</sub>' (mode-4) when none of the loads is powered. As a result, two loads are powered simultaneously while the third load receives no power. This procedure is performed in a cyclic pattern. Hence, this approach is known as 'cyclic control,' and it is depicted in Fig.2.

Average power supplied to the loads are expressed through equations (1)-(6) [16]

$$\text{Average power of load - 1, } P_1 = \frac{t_1 + t_2}{T} P_{max} \quad (1)$$

$$\text{Average power of load - 2, } P_2 = \frac{t_2 + t_3}{T} P_{max} \quad (2)$$

$$\text{Average power of load - 3, } P_3 = \frac{t_1 + t_3}{T} P_{max} \quad (3)$$

Load power during  $t_4$ ,  $P_4$  = zero

$$P_1 + P_2 + P_3 + P_4 = \frac{t_1 + t_2}{T} P_{max} + \frac{t_2 + t_3}{T} P_{max} + \frac{t_1 + t_3}{T} P_{max} \quad (4)$$

$$P_1 + P_2 + P_3 + P_4 = \frac{t_1 + t_2 + t_2 + t_3 + t_1 + t_3}{T} P_{max} \quad (5)$$

At specific instant, when  $t_1 = t_2 = t_3$  then load powers are equal  $P_1 = P_2 = P_3 = P_l$  and  $t_1 + t_2 + t_3 = T$

$$P_l = \frac{2}{3} P_{max} \quad (6)$$

TABLE I  
SIMULATION CIRCUIT PARAMETERS

Parameter	Value
AC input voltage ( $V_s$ )	50 V
Boost inductor	400 $\mu$ H
dc-link capacitor	6.8 $\mu$ F
IC load equivalent inductance ( $L_1, L_2, L_3$ )	62.03 $\mu$ H
IC load equivalent resistance ( $R_1, R_2, R_3$ )	2.22 $\Omega$
Load resonant capacitor ( $C_{r1}, C_{r2}, C_{r3}$ )	1.205 $\mu$ F
switching frequencys of legs ( $f_s$ )	50 kHz
IH load resonant frequency( $f_{rl}$ )	48.5 kHz
Snubber capacitors	2 nF

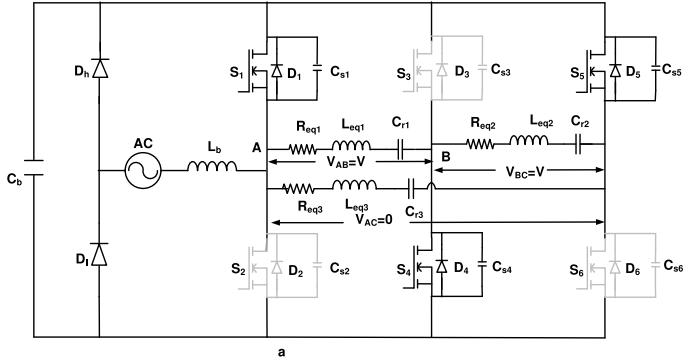


Fig. 3. Equivalent circuits For  $V_s > 0$  (Positive half cycle)  
 (a) Mode-1  $v_{g1}$ ,  $v_{g4}$  and  $v_{g5}$  are in phase  
 (b) Mode-2  $v_{g2}$ ,  $v_{g4}$  and  $v_{g5}$  are in phase  
 (c) Mode-3  $v_{g2}$ ,  $v_{g3}$  and  $v_{g5}$  are in phase  
 (d) Mode-4  $v_{g1}$ ,  $v_{g3}$  and  $v_{g5}$  are in phase

#### IV. SIMULATION WAVEFORMS

Simulation results of the proposed single-stage three leg converter configuration for three IC loads are shown in Fig.4

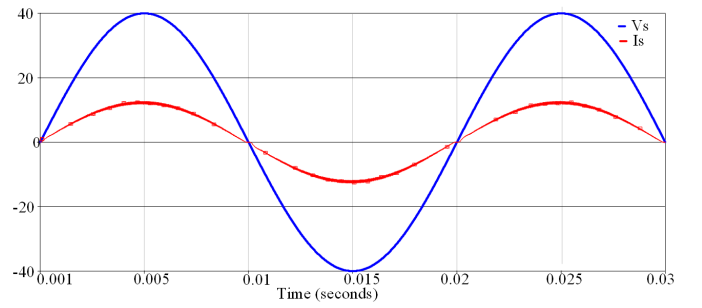


Fig. 4. Source Voltage( $V_s$ ) and Source Current ( $I_{02}$ )

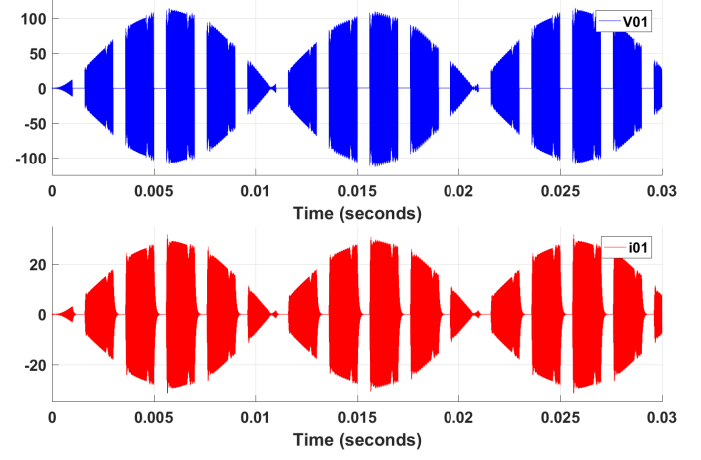
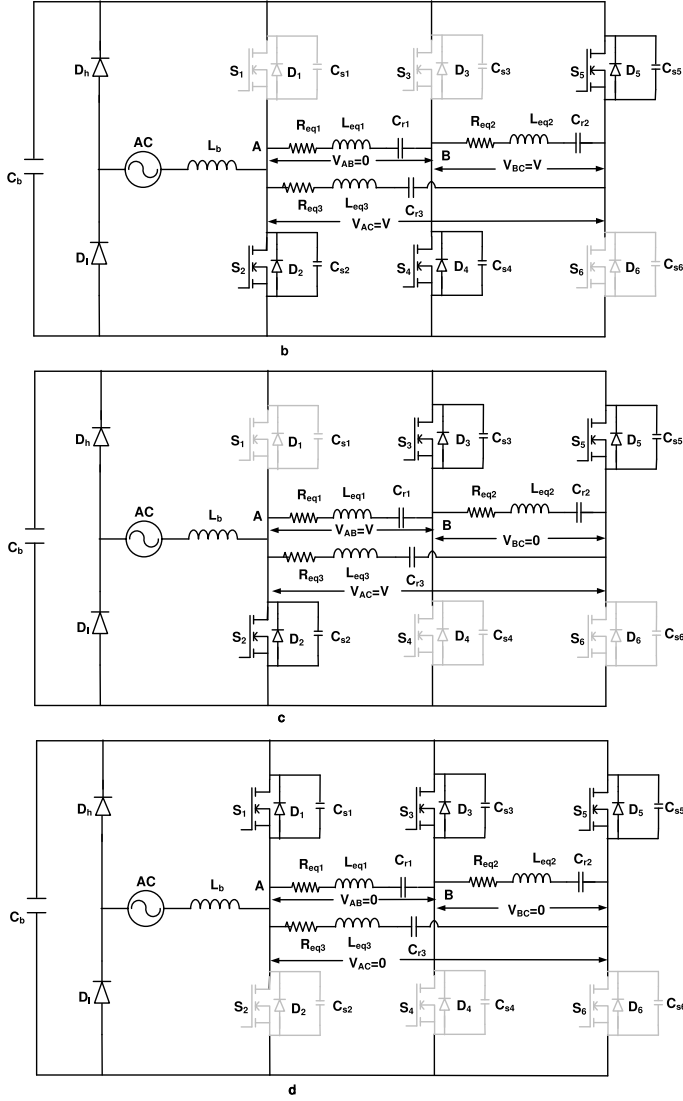


Fig. 5. Load-1 Voltage ( $V_{01}$ ) and Current ( $I_{01}$ ) at  $D_1 = 0.95$

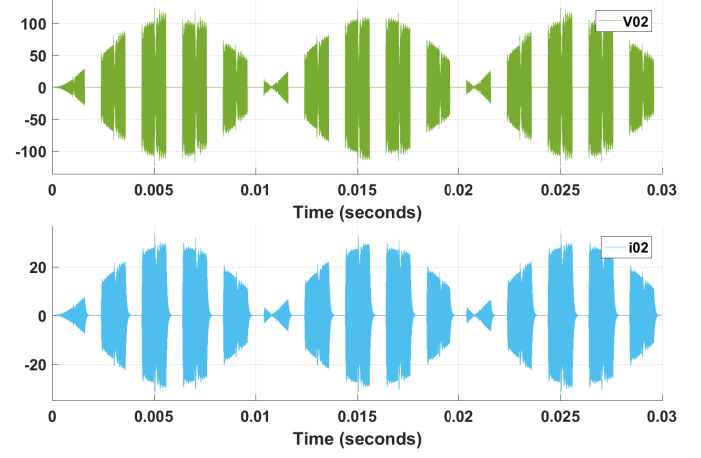


Fig. 6. Load-2 Voltage ( $V_{02}$ ) and Current ( $I_{02}$ ) at  $D_2 = 0.95$

to Fig.17. Individual load duty cycles are calculated based on load power requirement. Fig.4 shows source voltage and source current waveforms. From this figure it is observed that supply power factor is unity. Fig.5 to Fig.7 depict the simulation results with equal output powers of  $P_1 = 316$  W,  $P_2 = 316$  W, and  $P_3 = 316$  W. From the time periods  $t_1$ ,  $t_2$ ,  $t_3$ , and  $t_4$ , the duty cycles of the loads are computed as  $d_1 = 0.95$ ,  $d_2 = 0.95$ , and  $d_3 = 0.95$ . Fig.8 shows the zoomed waveforms of all three load voltages and load currents. The

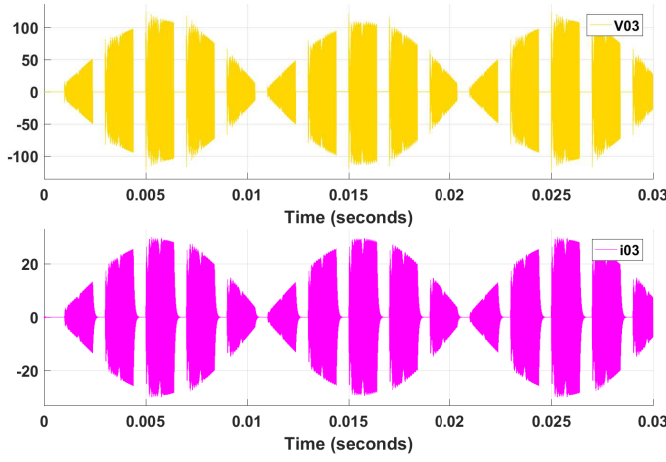


Fig. 7. Load-3 Voltage ( $V_{03}$ ) and Current ( $I_{03}$ ) at  $D_3 = 0.95$

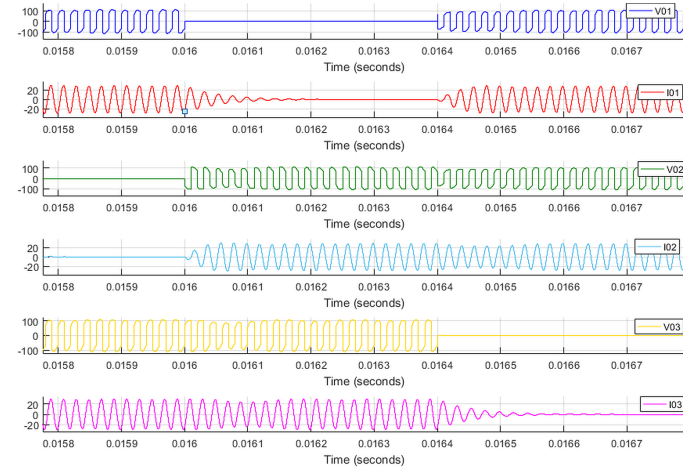


Fig. 8. Zoomed waveforms of load voltages and load currents

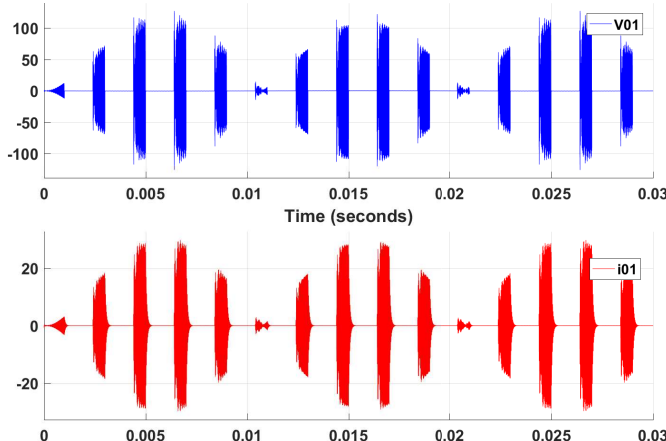


Fig. 9. Load-1 Voltage ( $V_{01}$ ) and Current ( $I_{01}$ ) at  $D_1 = 0.3$

simulation results with output powers of  $P_1 = 120$  W,  $P_2 = 316$  W, and  $P_3 = 316$  W is shown in Fig.9 to Fig.11. The duty cycle of the loads is determined as  $d_1 = 0.3$ ,  $d_2 = 0.95$ , and  $d_3 = 0.95$  from the time periods  $t_1$ ,  $t_2$ ,  $t_3$ , and  $t_4$ . The simulation

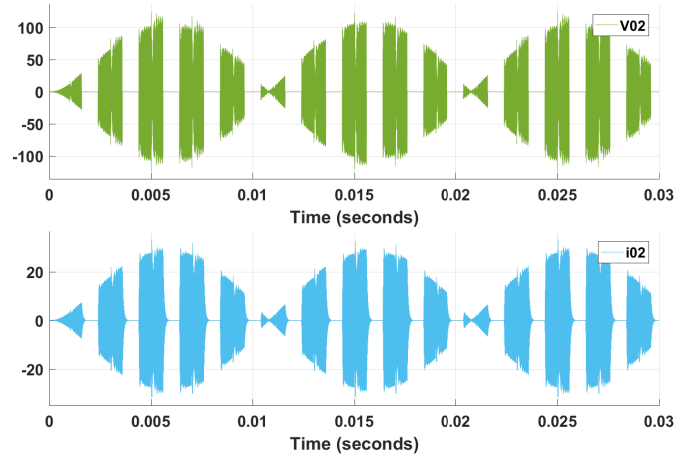


Fig. 10. Load-2 Voltage ( $V_{02}$ ) and Current ( $I_{02}$ ) at  $D_2 = 0.95$

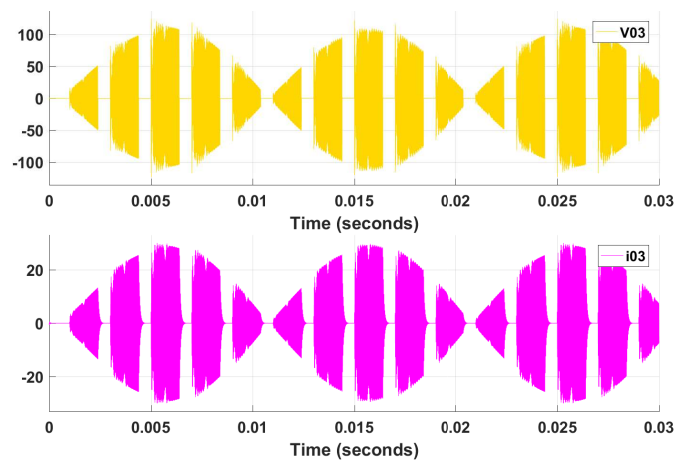


Fig. 11. Load-3 Voltage ( $V_{03}$ ) and Current ( $I_{03}$ ) at  $D_3 = 0.95$

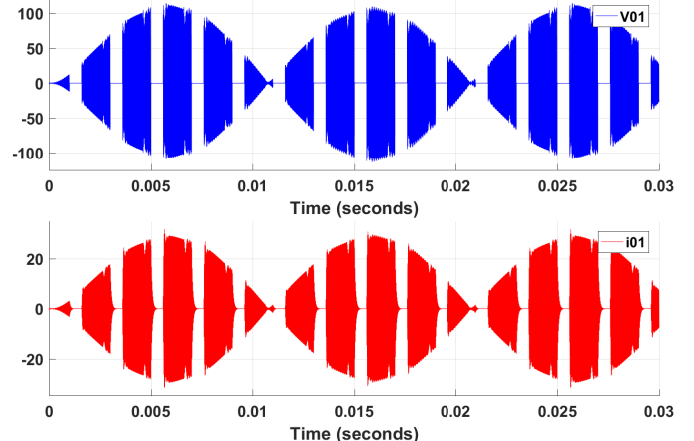


Fig. 12. Load-1 Voltage ( $V_{01}$ ) and Current ( $I_{01}$ ) at  $D_1 = 0.95$

results with output powers of  $P_1 = 316$  W,  $P_2 = 120$  W, and  $P_3 = 316$  W is depicted in Fig.12 to Fig.14. The duty cycle of the loads is determined as  $d_1 = 0.95$ ,  $d_2 = 0.3$ , and  $d_3 = 0.95$  based on the time periods  $t_1$ ,  $t_2$ ,  $t_3$ , and  $t_4$ . Fig.15 to Fig.17

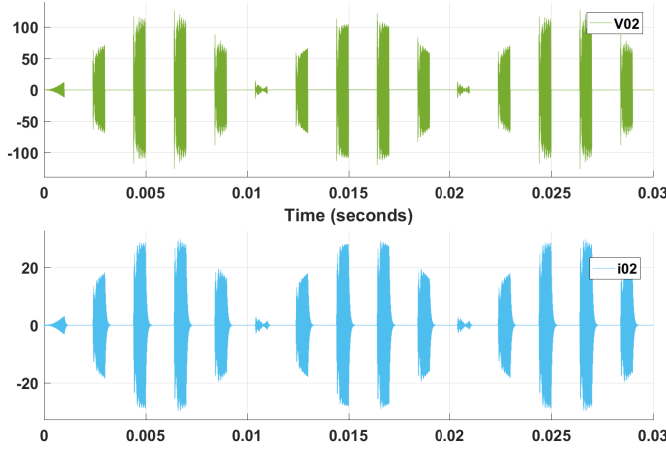


Fig. 13. Load-2 Voltage ( $V_{02}$ ) and Current ( $I_{02}$ ) at  $D_2 = 0.3$

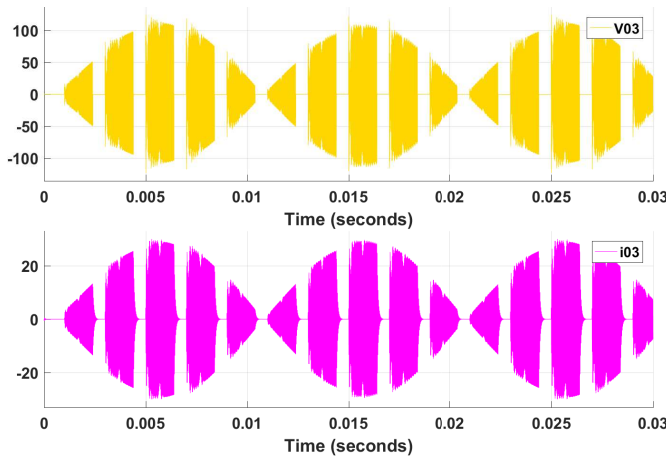


Fig. 14. Load-3 Voltage ( $V_{03}$ ) and Current ( $I_{03}$ ) at  $D_3 = 0.95$

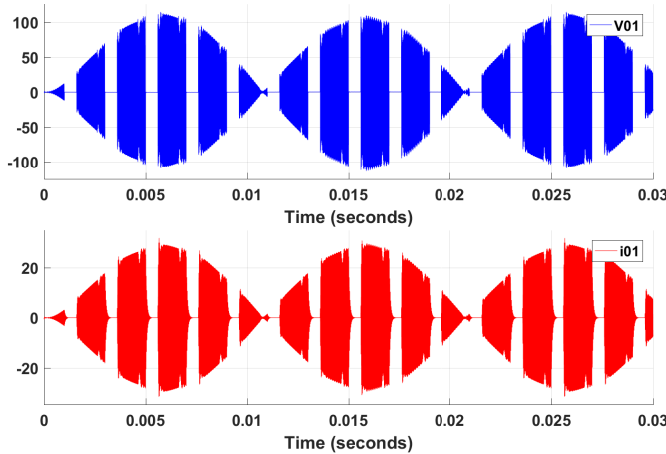


Fig. 15. Load-1 Voltage ( $V_{01}$ ) and Current ( $I_{01}$ ) at  $D_1 = 0.95$

show the simulation results with output powers of  $P_1 = 316$  W,  $P_2 = 316$  W, and  $P_3 = 120$  W. The duty cycle of the loads is determined as  $d_1 = 0.95$ ,  $d_2 = 0.95$ , and  $d_3 = 0.3$  from the time periods  $t_1$ ,  $t_2$ ,  $t_3$ , and  $t_4$ .

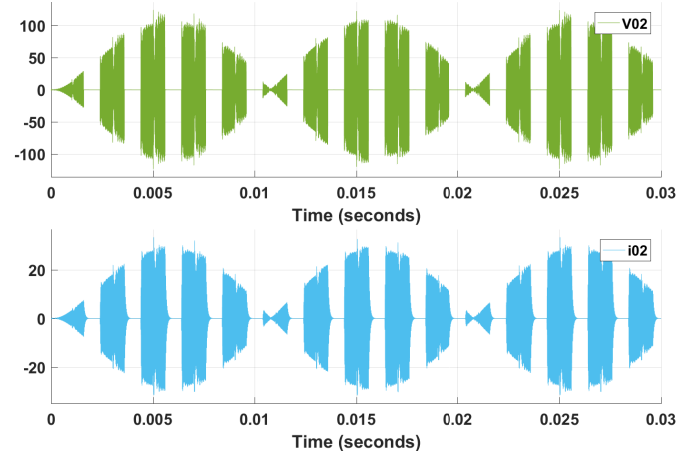


Fig. 16. Load-2 Voltage ( $V_{02}$ ) and Current ( $I_{02}$ ) at  $D_3 = 0.95$

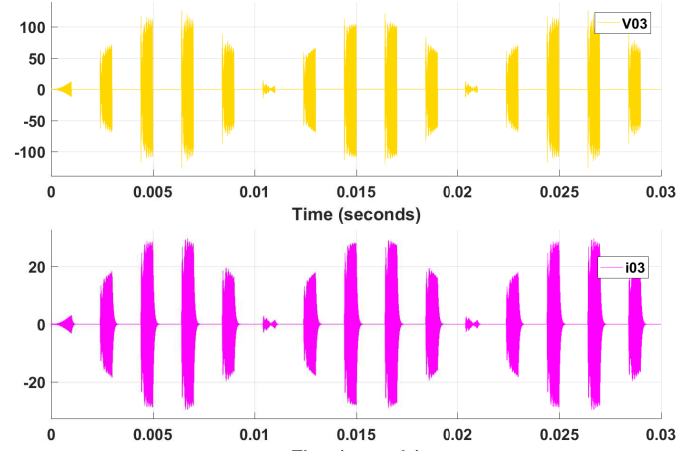


Fig. 17. Load-3 Voltage and Current at  $D_2 = 0.3$

Fig.18 presents independent load power regulation. According to Fig.18a, load-1 power varies with  $d_1$  while load-2 and load-3 powers remain constant with fixed  $d_2$  and  $d_3$ . According to Fig.18b, load-2 power varies  $d_2$  while load-1 and load-3 powers remain constant with fixed  $d_1$  and  $d_3$ . Similarly According to Fig.18c, load-3 power varies  $d_3$  while load-1 and load-2 powers remain constant with fixed  $d_1$  and  $d_2$ . At various power levels, the proposed resonant converter to obtain zero voltage or zero current during the switching period; if this desired feature is achieved, the switching power losses decreases to minimum, hence proposed converter achieves high efficiency ( $\geq 95\%$ ).

## V. CONCLUSIONS

In this paper, a cyclic controlled single-stage three-leg resonant converter for three output domestic IH applications is proposed. The converter offers bridge less rectifier operation, input power factor correction, boost operation, ZVS and operates at fixed switching frequencies. All three IH loads are regulated simultaneously and independently. The developed approach has fewer components and provides one leg per

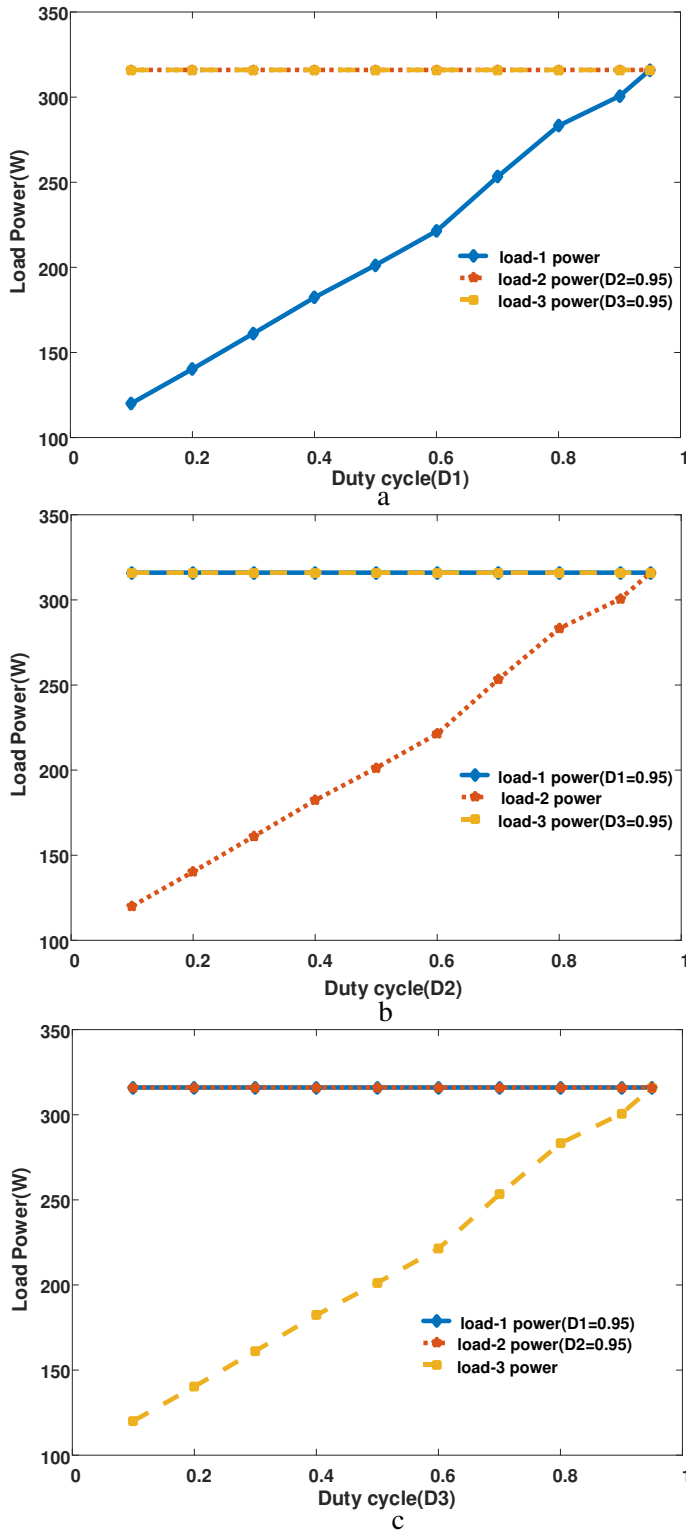


Fig. 18. independent Power control of loads (a) load-1 power control (b) load-2 power control (c) load-3 power control

load on average. It may also be expanded to accommodate more than three loads. The simulation results are presented. The proposed converter's design and control are simple, cost

effective, and efficient.

## REFERENCES

- [1] O. Lucía, P. Maussion, E. J. Dede, and J. M. Burdío, "Induction heating technology and its applications: past developments, current technology, and future challenges," *IEEE Transactions on industrial electronics*, vol. 61, no. 5, pp. 2509–2520, 2013.
- [2] E. Plumed, J. Aceró, I. Lope, and J. M. Burdío, "Design methodology of high performance domestic induction heating systems under worktop," *IET Power Electronics*, vol. 13, no. 2, pp. 300–306, 2020.
- [3] L. Meng, K. W. E. Cheng, and K. W. Chan, "Systematic approach to high-power and energy-efficient industrial induction cooker system: circuit design, control strategy, and prototype evaluation," *IEEE transactions on power electronics*, vol. 26, no. 12, pp. 3754–3765, 2011.
- [4] H. Sarnago, O. Lucía, A. Mediano, and J. Burdío, "Analysis and design of high-efficiency resonant inverters for domestic induction heating applications," *International Journal of Applied Electromagnetics and Mechanics*, vol. 44, no. 2, pp. 201–208, 2014.
- [5] F. Forest, E. Labouré, F. Costa, and J. Y. Gaspard, "Principle of a multi-load/single converter system for low power induction heating," *IEEE Transactions on Power Electronics*, vol. 15, no. 2, pp. 223–230, 2000.
- [6] D. Vijaya Bhaskar, N. Vishwanathan, T. Maity, and S. Porpandiselvi, "A three-output inverter for induction cooking application with independent control," *EPE Journal*, vol. 28, no. 2, pp. 89–99, 2018.
- [7] T. Ahmed, K. Ogura, S. Chandhakar, and M. Nakaoka, "Asymmetrical duty cycle controlled edge resonant soft switching high frequency inverter for consumer electromagnetic induction fluid heater," *Automatica*, *ATKAAF*, vol. 44, no. 1-2, pp. 21–26, 2003.
- [8] S. Khatroth and P. Shunmugam, "Cascaded full-bridge resonant inverter configuration for different material vessel induction cooking," *IET Power Electronics*, vol. 13, no. 19, pp. 4428–4438, 2020.
- [9] S. Komeda and H. Fujita, "A phase-shift-controlled direct ac-to-ac converter for induction heaters," *IEEE Transactions on Power Electronics*, vol. 33, no. 5, pp. 4115–4124, 2017.
- [10] V. Esteve, J. Jordán, E. Sanchis-Kilders, E. J. Dede, E. Maset, J. B. Ejea, and A. Ferreres, "Enhanced pulse-density-modulated power control for high-frequency induction heating inverters," *IEEE Transactions on Industrial Electronics*, vol. 62, no. 11, pp. 6905–6914, 2015.
- [11] H. Sarnago, O. Lucía, M. Pérez-Tarragona, and J. M. Burdío, "Dual-output boost resonant full-bridge topology and its modulation strategies for high-performance induction heating applications," *IEEE Transactions on Industrial Electronics*, vol. 63, no. 6, pp. 3554–3561, 2016.
- [12] H. Sarnago, O. Lucia, A. Mediano, and J. M. Burdío, "Design and implementation of a high-efficiency multiple-output resonant converter for induction heating applications featuring wide bandgap devices," *IEEE Transactions on Power Electronics*, vol. 29, no. 5, pp. 2539–2549, 2013.
- [13] H. Sarnago, O. Lucia, and J. M. Burdío, "Multiple-output boost resonant inverter for high efficiency and cost-effective induction heating applications," in *2016 IEEE Applied Power Electronics Conference and Exposition (APEC)*. IEEE, 2016, pp. 1040–1044.
- [14] M. Pérez-Tarragona, H. Sarnago, O. Lucía, and J. M. Burdío, "Design and experimental analysis of pfc rectifiers for domestic induction heating applications," *IEEE Transactions on Power Electronics*, vol. 33, no. 8, pp. 6582–6594, 2017.
- [15] S. Khatroth and P. Shunmugam, "Single-stage pulse frequency controlled ac-ac resonant converter for different material vessel induction cooking applications," *International Journal of Circuit Theory and Applications*, 2021.
- [16] H. Sarnago, O. Lucia, and J. Burdío, "Multiple-output zcs resonant inverter for multi-coil induction heating appliances," in *2017 IEEE Applied Power Electronics Conference and Exposition (APEC)*. IEEE, 2017, pp. 2234–2238.
- [17] R. C. M. Gomes, M. A. Vitorino, D. A. Acevedo-Bueno, and M. B. de Rossiter Corrêa, "Multiphase resonant inverter with coupled coils for ac-ac induction heating application," *IEEE Transactions on Industry Applications*, vol. 56, no. 1, pp. 551–560, 2019.
- [18] O. Lucia, C. Carretero, J. M. Burdío, J. Aceró, and F. Almazan, "Multiple-output resonant matrix converter for multiple induction heaters," *IEEE Transactions on Industry Applications*, vol. 48, no. 4, pp. 1387–1396, 2012.